NASA TECHNICAL MEMORANDUM

NASA TM X-3366

NASA TM X-3366

NOISE SUPPRESSION BY AN ACOUSTICALLY TREATED THREE-RING INLET ON A TF-34 ENGINE

Gene L. Minner, Richard G. Goldman, and Laurence J. Heidelberg

Lewis Research Center
Cleveland, Ohio 44135

NATIONAL AERONAUTICS AND SPACE ADMINISTRATION • WASHINGTON, D. C. • MARCH 1976

1. Report No.	2. Government Accession No.	3. Recipient's Catalog No.
NASA TM X-3366		

4. Title and Subtitle
NOISE SUPPRESSION BY AN ACOUSTICALLY TREATED THREE-RING INLET ON A TF-34 ENGINE

5. Report Date
March 1976

6. Performing Organization Code

7. Author(s) Gene L. Minner, Richard G. Goldman, and Laurence J. Heidelberg

8. Performing Organization Report No.
E-8524

10. Work Unit No.
505-03

9. Performing Organization Name and Address
Lewis Research Center
National Aeronautics and Space Administration
Cleveland, Ohio 44135

11. Contract or Grant No.

13. Type of Report and Period Covered
Technical Memorandum

12. Sponsoring Agency Name and Address
National Aeronautics and Space Administration
Washington, D.C. 20546

14. Sponsoring Agency Code

15. Supplementary Notes

16. Abstract

Acoustic performance tests were conducted with a three-ring inlet noise suppressor designed for a TF-34 engine. For all tests the aft noise sources were highly suppressed. The measured inlet suppression was large, reaching levels greater than 30 dB at the peak. Comparisons of the data and the performance predictions were in reasonably good agreement. The frequency of peak attenuation was well predicted; the magnitude and spectral shape were reasonably well predicted. The agreement was best when the distribution of sound energy across the inlet was taken into account in the performance predictions. Tests in which the length of treatment was varied showed an orderly progression of attenuation with length. The performance predictions for the different lengths also showed an orderly progression with length. At the highest speed of the engine, multiple pure tones were present throughout the spectrum in the source noise signature. These tones were effectively suppressed by the inlet liner, even at low frequencies, although the liner was designed to work best at the blade-passing frequency.

17. Key Words (Suggested by Author(s))	18. Distribution Statement
Acoustic suppression; Inlet suppressor; Splitter rings; Engine acoustics; Aircraft noise; Noise abatement	Unclassified - unlimited STAR Category 71

19. Security Classif. (of this report)	20. Security Classif. (of this page)	21. No. of Pages	22. Price*
Unclassified	Unclassified	37	$3.75

* For sale by the National Technical Information Service, Springfield, Virginia 22161

NOISE SUPPRESSION BY AN ACOUSTICALLY TREATED THREE-RING INLET ON A TF-34 ENGINE

by Gene L. Minner, Richard G. Goldman, and Laurence J. Heidelberg

Lewis Research Center

SUMMARY

Acoustic performance tests were conducted with a three-ring inlet noise suppressor designed for a TF-34 engine. For all tests the aft noise sources were highly suppressed. The measured inlet suppression was large, reaching levels greater than 30 decibels at the peak. Comparisons of the data and performance predictions were in reasonably good agreement. The frequency of peak attenuation was well predicted. The agreement was best when the distribution of sound energy across the inlet was taken into account in the performance predictions. Tests in which the length of treatment was varied showed an orderly progression of attenuation with length. The performance predictions for the different lengths also showed an orderly progression with length. At the highest speed of the engine, multiple pure tones were present throughout the spectrum in the source noise signature. These tones were effectively suppressed by the inlet liner, even at low frequencies, although the liner was designed to work best at the blade-passing frequency.

INTRODUCTION

A full scale TF-34 engine has been used at the Lewis Research Center as a test bed for noise reduction concepts for STOL (short takeoff and landing) and short-haul aircraft. The overall test program on this engine has included inlet noise, exhaust noise, jet noise and lift augmentation system noise. All of these noise sources must be controlled in order to meet noise goals of the future.

Goals for acceptable noise levels for future aircraft are expected to become increasingly difficult to meet. In particular, STOL noise requirements will be stringent because of anticipated operations near population centers. Therefore, greater reductions of engine noise will be required than for conventional aircraft.

This report deals with the suppression of internally generated engine noise that escapes from the engine inlet. To achieve the necessary large noise reductions, a large amount of acoustic treatment was placed in the inlet, on three splitter rings and on the cowl wall. The acoustic treatment was designed to produce its peak noise reduction at the fan blade-passing tone frequency at high engine speed. It was also desired to achieve large noise reductions at several one-third-octave frequency bands on either side of the peak. The actual noise reduction resulting from this inlet acoustic treatment was determined by comparing its measured far-field noise against the measured noise from an inlet with no rings and with the wall treatment taped. Also tested was an inlet configuration with all rings in place but with all treated surfaces taped over to simulate the hard-wall condition (no treatment). This configuration with hard rings could be used as an alternate baseline to evaluate the effect of activating the rings.

To examine the relationship between noise reduction and the amount of acoustic treatment, several different lengths of treatment were tested. These length variations were achieved by placing tape over selected lengths of the acoustic treatment.

Some tests of a similar nature were performed at Edwards Air Force Base, and the results were presented in references 1 and 2. The engine configurations tested at Lewis differed from those at Edwards in two essential features: First, the present tests included length variations, and, second, the present tests excluded the engine rear-end noise as a factor in the measured inlet-noise data. The second feature resulted from the placement of an extended noise suppressor on the engine exhaust, which suppressed the aft turbomachinery and jet noise.

This report is organized primarily around the measured results of the noise reduction tests. Experimental results of far-field noise measurements are presented for a baseline engine configuration (no acoustic treatment) and for acoustically treated configurations. The far-field data are presented as angular distributions of sideline PNL (perceived noise level), as one-third-octave-band frequency spectra of SPL (sound pressure level) at the maximum PNL angle, as frequency spectra of PWL (sound power level), and as spectra of PWL suppression. Also included is a limited amount of inlet in-duct spectral data. These data take the form of narrow-band and one-third-octave-band frequency spectra at selected internal locations.

The report also discusses the original acoustic treatment design philosophy and compares the measured far-field noise suppression PWL spectra and calculated estimates of the noise suppression spectra made using the methods of reference 3.

APPARATUS AND PROCEDURE

Engine

The TF-34 ground-test engine used for this test series was described in detail in

references 1 and 4. As shown in figure 1, there is one major difference between the complex sound source of the engine of references 1 and 4 and the engine installed for the present program. That difference is the addition of an 18.3-meter (60-ft) long, 1.68-meter (66-in.) inside-diameter tailpipe muffler on the engine (fig. 2). This muffler was lined with a 59-centimeter ($23\frac{1}{4}$-in.) deep bulk absorber (shielded by a perforated steel plate), which effectively eliminated aft-radiated and jet noise from consideration at the inlet-hemisphere microphone locations used for the inlet tests.

The engine test conditions included several speeds from about 5100 to 6900 rpm for most configurations. For the purpose of assessing the capabilities of the inlet suppressor performance, two speeds have been selected for presentation here: 5100 rpm was representative of low-speed acoustic behavior, and 6200 rpm was representative of high speed behavior where multiple pure tones are present. Some basic design parameters of the engine and its performance are given in table I. A more detailed description appears in reference 4.

Inlet Acoustic Treatment Design

The inlet splitter-ring acoustic treatment configuration was designed using a combination of theoretical and experimental information. The suppressor was designed by adjusting its parameters so that a calculated attenuation spectrum, when subtracted from the engine noise source spectrum, would yield a predetermined PNL. The peak of the attenuation spectrum was calculated from curves relating attenuation and liner parameters. The functional dependence of the peak attenuation on the design parameters was theoretically determined. The level of the function was determined using measured experimental results from fan suppressor tests (from ref. 5). The off-peak behavior was determined using a curve drawn through a set of experimental data (refs. 5 to 7). The required wall impedance was calculated from plane-wave theory with a velocity continuity boundary condition; the wall geometry was selected to yield this value of impedance using a model that relates wall impedance to wall geometry.

The three-ring inlet suppressor is shown in figure 3. All acoustic treatment is of a single construction, namely, a 6.8-percent-open area-ratio, 0.051-centimeter (0.020-in.) thick perforated face plate with a 0.127-centimeter (0.05-in.) diameter hole size and a 1.22-centimeter (0.480-in.) honeycomb treatment depth. The radial spacing between treated surfaces of the annular passages was 11.4 centimeters (4.5 in.), except for the innermost passage, which was cylindrical with a 24.1-centimeter (9.5-in.) diameter. The part of the acoustic treatment on the duct wall extending axially beyond the rings was not part of the original design but was placed there to allow the axial translation of the splitter-ring assembly (fig. 3) by using the multiple mounting points

of the ring support. By thus extending the outer wall treatment, the outer passage was lined on both surfaces at all times. In tests performed elsewhere (ref. 1) the axial location of the rings had no observable effect on the noise reduction. The experimental results labeled "fully treated inlet" in this report are for the configuration with this extended outer wall treatment acoustically active. Other results herein, including performance predictions, are for configurations with the portion of the outer wall treatment that extends beyond the extremities of the rings made acoustically inactive.

The original design was intended to yield a peak attenuation of about 32 decibels at the blade-passing frequency in the 3150-hertz one-third-octave band. Because of changes in design theory since that time (notably the Mach number effect on optimum impedance), both the level and the frequency are predicted to be different than these values, thus the peak frequency is now predicted to be near 2000 hertz, as will later become apparent.

In addition to the three-ring inlet suppressor (fig. 3) three other treated configurations were tested. These were different in the amount of acoustic treatment left active (fig. 4). The lengths tested were nominally 17.8 centimeters (7.0 in.), 36.8 centimeters (14.5 in.), and full length active in each passage. Because the passages are not the same, the effective treatment lengths in these passages differ from the nominal values given. For example, parts of the treatment in passage III are opposed by acoustically hard surfaces that perform differently from the soft-opposed-by-soft cases.

To assess the noise attenuation performance of the treated configurations, two baseline configurations were tested. The first of these configurations has no splitter rings and taped acoustic treatment on the walls (baseline inlet). The second was a deactivated fully treated inlet (wall treatment, three splitter rings); that is, all acoustically treated surfaces were taped (simulated baseline inlet). The baseline configuration was used to evaluate the effect of the rings and the acoustic treatment on the rings and walls. The simulated baseline configuration could be used to examine the noise reduction resulting from activating the acoustic treatment.

Test Facility and Instrumentation

The engine configuration and inlet ducting were supported from above by a cantilevered support arm with the engine centerline 2.7 meters (9.0 ft) above the ground plane (fig. 2). The ground surface at the test site was smooth concrete over most of its area, with a section of asphalt pavement extending beyond the microphone array.

A plan view of the site (fig. 5) shows the placement of far-field microphones on a 30.5-meter (100-ft) radius arc, centered on the engine tailpipe. Various combinations of these microphones were tested, with placement at the ground level and at the engine

centerline height. The availability of data processing channels limited the number of microphones that could be used; thus not all measurement locations could be recorded simultaneously. The results presented herein for the baseline and fully treated inlet configurations are from a set of microphone locations at the engine centerline height, with microphones at 10^{o} increments on the noted arc. The results of the remaining treated configurations were from the same microphone array, except that the 10^{o} and 30^{o} microphones were omitted.

As it was set up for more general investigations, the microphone arc was arranged assuming an aft noise source, and the center of the arc is located there. For the present tests the noise source was located at the inlet plane of the bellmouth, since the muffler suppressed the aft noise. Accordingly, calculation of sound power levels was made relative to the inlet source location. The data processing computer was programmed to calculate sound pressure levels on a corrected 30.5-meter (100-ft) radius arc centered on the engine inlet and at microphone angular positions relative to this new center. The correction involved a mathematical translation of coordinates in which the origin was moved along the centerline of the engine from the aft end to the inlet plane. The distance of translation was 6.98 meters (22.9 ft).

The readings from the 1.26-centimeter (0.5-in.), far-field, condenser microphones were processed on-line through the standard Lewis one-third-octave-band data-reduction system. (See, e.g., ref. 5.) Selected microphones were tape recorded. The method of calculating sound levels at locations other than the measurement stations was consistent with the methods of reference 8. Power levels were calculated assuming an axisymmetric source and integrating the far-field sound intensity over the inlet hemisphere. Thus no attempt was made to correct the results to free-field conditions. The ground reflection effect is a complex phenomenon dependent on frequency. On the average, however, the presence of the ground plane reflects extra energy to the microphones. Ignoring this effect may therefore produce absolute levels that are high, but it should not affect comparisons of different configurations reported here. By integrating only over the inlet hemisphere, the effect on the results of any residual noise escaping from the aft muffler is minimized.

In addition to the far-field sound data, limited in-duct measurements were taken. Acoustic probes were traversed radially at two different axial locations. Figure 6 shows these locations. These probes were of the infinite tube type described in reference 2. The arrangement was calibrated to provide true amplitude and frequency readouts. The PT-1 probe was located 64 centimeters (25 in.) upstream of the rings' leading edges, and the PT-2 probe was located 5 centimeters (2 in.) downstream of the outer rings' trailing edges, with a sensing tap 25 centimeters (10 in.) upstream of the leading edge of the fan blade at the tip. Both probes provided a spectral data at selected radial locations for a few engine speeds. The locations for PT-1 were the centers of passages I, II,

and IV. Probe PT-2 locations were the centers of passages I and II and directly behind the trailing edge of the inner ring, which was removed when PT-2 was used. The travel at this location was restricted by the centerbody. The probe readings were processed through a narrow-band frequency analyzer. These narrow-band spectra have also been converted by calculation to one-third-octave band spectra for presentation in this report.

PRESENTATION AND DISCUSSION OF MEASURED RESULTS

The acoustic performance of several variations of a three-ring inlet-noise suppressor on a full-scale TF-34 engine was measured. Different amounts of active suppression material, achieved by varying the amount of tape placed over parts of the full inlet liner produced these variations. The tests were run with the engine at several speeds. Two fan speeds, nominally 5100 and 6200 rpm, were selected for presentation of data as being typical of low-speed and high-speed performance.

The acoustic data include sound levels measured by probes inside the duct and by stationary far-field microphones. The far-field data are more extensive and are presented first. Multiple data samples (generally two or three) were measured in the far field for most cases. Variations in the spectra from one sample to another were generally less than 1 decibel.

All measurements were made at the microphone locations discussed in the section Test Facility and Instrumentation. Data presented herein at other locations have been adjusted from the true measured values by accounting for distance and atmospheric absorption effects.

Perceived Noise Levels and Maximum Angle Spectra

For STOL applications a commonly used format for noise projections is the variation of PNL along a 152.5-meter (500-ft) sideline. This gives a good indication of the perceived noise signature of the device. The PNL values presented in this report are those along the sideline of a single TF-34 engine with the aft noise eliminated by a very effective massive exhaust suppressor.

Figure 7 presents the PNL variation for the nominal 5100 and 6200 rpm fan speeds, respectively. Included in the figure are the data for the baseline inlet engine and the data for the fully treated-inlet engine. (See fig. 3 for details of the fully treated inlet, which included the extended outer-wall treatment.) Incidentally, figure 7 shows that the rear-end noise levels (large angles) are notably lower than the front end levels because of the large amount of rear end suppression. By contrast, the results given in refer-

ence 1 show two humps in the PNL curve. There, the rear-end noise was not so effectively reduced.

All the data in figure 7 have the peak of the PNL directionality pattern at about 50° to 60° from the inlet. The fully treated inlet greatly reduced noise at all angles. The reduction at the peak noise angle was about 15 perceived noise decibels (PNdB) at 5100 rpm and 19 PNdB at 6200 rpm. At the angles furthest from the inlet, there was about a 10-PNdB reduction. Examination of PNL at 5800, 6500, and 6900 rpm fan speeds revealed quite similar behavior.

Note that the angles in figure 7 are not evenly spaced. This spacing is a result of the placement of the center of the microphone arc as discussed in connection with figure 5. If the microphones in their actual locations were equally spaced on an arc centered on the engine exhaust, then obviously they were not equally spaced on an arc centered on the effective source - the inlet. This factor has been considered in processing the data relative to the inlet sound source.

To establish a more detailed understanding of the sound source, one-third-octave band spectra of SPL are shown in figure 8 at 5100 and 6200 rpm for the baseline inlet and fully treated inlet engines. The location chosen is the angle of maximum sideline PNL, but the SPL data are presented on a 30.5-meter (100-ft) radius to reduce the effect of atmospheric absorption on the high-frequency bands. At 5100 rpm figure 8(a) shows a baseline spectrum typical of engine fans at low tip speed, dominated by the blade-passage tone (2500-Hz band) and its harmonic (5000-Hz band). There is little evidence of jet noise at either 5100 or 6200 rpm, as would be expected with the extended aft muffler. The spectrum of the fully treated inlet shows that suppression was achieved from about 630 to 10 000 hertz. As will later be discussed the frequency of peak attenuation is predicted to be near 2000 hertz. At some frequencies the fully treated level is above the baseline engine noise level. In nearly all cases the amount of this apparent "extra noise" is small. This effect may result either from uncertainties in the data or from some extra noise generation by the liner at these frequencies. Similar behavior was observed in the data of reference 9. It is not possible to resolve this issue with the present data. The noise reduction at the blade-passage frequency (2500 Hz) was over 30 decibels, while the reduction at the second harmonic was about 15 decibels.

The baseline inlet noise spectrum at 6200 rpm (fig. 8(b)) is significantly different from that at 5100 rpm. The main difference is due to the presence of buzz-saw noise or MPT's (multiple pure tones) typical of higher tip speed fans. These MPT's dominate the spectrum at 6200 rpm, to the extent that the blade-passage tone is no longer identifiable as a spike in the one-third-octave band spectrum. Results presented in reference 1 for a 7100-rpm fan speed, by contrast, showed spikes in the spectrum at the blade-passage frequency and its higher harmonics. This apparent conflict may originate from a speed effect, or it may be due to differences in the engine installations at Edwards and Lewis.

The spectrum for the fully treated inlet follows the baseline spectrum at low and high frequencies. At the higher speed the peak suppression occurs at a somewhat lower frequency than the blade-passage frequency. Such a shift would also be predicted theoretically for increasing Mach numbers over inlet liners. In addition the MPT's may be more easily removed because of amplitude and/or modal effects peculiar to MPT's.

Inlet Sound Power Level Spectra

Calculations of noise reductions from theory are most readily related to the sound in the far field in terms of PWL. Calculating estimates of SPL reductions in the far field would require considerably more analysis including assumptions concerning sound radiation directionality from the inlet. Therefore, to set the stage for comparisons between estimated and measured liner performance, this section presents measured inlet PWL one-third-octave band spectra for several configurations at 5100 and 6200 rpm.

Figure 9 presents the PWL one-third-octave spectra at 5100 and 6200 rpm for the baseline inlet and for the fully treated inlet of figure 3. The same type of presentations as shown in figure 9 could be made for all of the treated configurations tested; instead, the results for those configurations are presented specifically as sound power level attenuation spectra.

The behavior of the PWL spectra shown in figure 9 is similar to the SPL spectra shown in figure 8. The magnitudes of the peak PWL noise reductions are quite similar to the SPL reductions at the angle of peak noise. Therefore, it may be reasonable to assume that calculations of liner performance, which are in terms of PWL reduction, can be applied directly to peak angle SPL spectra to estimate suppressed perceived noise levels. Such an explanation of the behavior is certainly a simplification, but may be a valid assumption for the present data, as a comparison of figures 8 and 9 seems to indicate.

The three-ring simulated baseline inlet could have been selected for these comparisons with the treated configurations. (This is the three-ring, fully taped configuration.) But the no-ring baseline configuration was selected because the total insertion effect of the rings was of primary interest. Nevertheless, for completeness we compare (fig. 10) the PWL spectra at 5100 and 6200 rpm of the baseline inlet with the simulated baseline inlet. The three-ring baseline spectrum at 5100 rpm is shifted upward from the no-ring hard-wall spectrum except at the blade-passage tone. It is possible that the taped splitters could cause extra noise generation, perhaps resulting from strut wakes or boundary-layer and ring-wake turbulence. At 6200 rpm there is no consistent shift of the spectrum. There is a crossover. Again, there may be extra noise generated at some frequencies by the splitter rings or the presence of the rings may alter the MPT

shock propagation and spectral development characteristics. As a result there appears to be less energy in MPT's and more in the blade-passage tone for the hard ringed case. This observation suggests that, when the acoustic treatment on the rings is active, it receives help in reducing the MPT noise through alteration of the untreated noise spectrum due to the mere presence of the rings.

For the comparisons of estimated and measured noise reductions, the sound power attenuation spectra for each treated configuration were taken relative to the baseline power level spectrum at the same engine speed.

In-Duct Narrow Band Sound Pressure Level Spectra

As noise reduction requirements become more stringent, more complete knowledge of the sound field in the engine duct will be required to allow the best design of acoustic suppressors. Not only does the distribution of sound influence where treated surfaces should be placed, but also the sound pattern (modal characteristics) has a strong influence on how much suppression can be anticipated, and it has a strong influence on the choice of the proper acoustic wall design (ref. 10).

The limited duct data taken in the present inlet test series certainly do not provide all of the information needed to properly design an advanced suppressor. Rather, the results presented here give a general indication of sound behavior in the duct of this specific engine. These in-duct results are useful for estimating the present liner performance. It is important to be aware that several pitfalls exist in making and interpreting these measurements. Three of these pitfalls are that aerodynamic turbulence impinging on the probe yields measurements that seem like sound, that the presence of the probe can cause extra noise generation, and that sound measurements made in the acoustic near field will likely yield erroneous data. The first and third of these conditions can lead to higher measured sound data than would be observed in the far field because these pseudosounds do not propagate to the far field. With increasingly sophisticated techniques, such erroneous measurements could be eliminated. The present data were taken disregarding these factors, for the most part. Therefore, some caution should be exercised in interpreting the data.

Narrow-band (20-Hz nominal bandwidth) SPL spectra from the PT-2 probe (fig. 6) with the engine at 5100 rpm are presented in figure 11 at radial locations 5.7, 20, and 41 centimeters (2.25, 8, and 16.12 in.) from the outer duct wall. These data were taken in a configuration that had the two outer rings in place and acoustically active. The measurements should be indicative of sound levels at the given axial location (see fig. 6) for all cases in the present tests, since at that axial location the sound has not encountered a significant amount of acoustic treatment.

The predominant features of the spectra of figure 11 are the tones that extend above the background levels by about 20 decibels. The tone at 425 hertz appears to be the fifth harmonic of the shaft rotative frequency. There are many weaker spikes distributed throughout the spectrum. These spikes occur at multiples of the shaft rotative frequency, which is 85 hertz. The same type of behavior for other transonic fans was reported in reference 11. The strong tones at higher frequencies are the blade-passing tone (2340 Hz) and its higher harmonics. Comparisons of figures 11(a), (b), and (c) show that there is some radial variation of the blade-passing tone and the harmonics, with the lowest levels occurring nearest the engine centerline.

Figure 12 shows narrow-band SPL spectra for 6200 rpm with probe PT-2 at the same radial stations as figure 11. The spectra at 6200 rpm are significantly different from those at 5100 rpm. At 6200 rpm there are a large number of strong tones throughout the spectrum at multiples of the shaft rotative frequency. These are the multiple pure tones, mentioned earlier, characteristic of supersonic fans. As was the case at 5100 rpm there is a strong tone at the fifth harmonic of the shaft frequency, in this case 520 hertz. The blade-passing tone at about 2800 hertz is clearly distinguishable, but the harmonics do not stand out significantly from the other adjacent tones. There is a significant change in the spectrum in passing from near the outer wall toward the center of the duct. The MPT's diminish in magnitude by a sizable amount. This result might be expected since the MPT's are believed to be associated with aerodynamic shock patterns at the blade tips, where the relative Mach number is the highest. A similar result for a different transonic fan was shown in reference 9.

At the upstream acoustic probe location (PT-1) data were taken for the three-ring simulated baseline inlet and for the fully treated inlet. The radial measurement positions were 5.7, 20, and 49.9 centimeters (2.25, 8, and 19.62 in.) from the outer wall. These positions correspond to the radial midpassage positions for the I, II, and IV passages.

Figure 13 presents the SPL narrow-band spectra at baseline 5100 rpm for the fully treated and three-ring simulated inlet configurations at the three radial locations. The simulated baseline spectra are similar to those measured by probe PT-2 (fig. 11) although the multiples of the shaft rotative frequency are not nearly so strong at PT-1. Comparison of the soft and hard configuration spectra shows significant SPL reductions over most of the spectra by the treatment, in particular it is remarkable that the blade-passing tone is reduced to the broadband level. The low-frequency soft-wall levels, however, are above the hard-wall levels. (Note: the logarithmic frequency scale tends to accentuate the low-frequency part of the spectrum.) This effect was observed in the far field; and, as was discussed earlier, it may indicate a noise generation problem caused by the liner. However, the far-field noise data for the treated configuration did not exceed the data for the taped configuration by such large amounts. Not all of the duct apparent extra noise reaches the far field as sound.

The SPL narrow-band spectra at PT-1 at 6200 rpm are shown in figure 14 for the three-ring, baseline inlet and fully taped inlet configurations. At this axial location the spectra are still characterized by strong MPT's, but these tones are not nearly as strong as those at PT-2 (fig. 12). This observation probably indicates that probe PT-2 was located in the near field of these tones where pseudosound was being measured. Again, the fully treated configuration has lower sound levels over most of the spectra, except at low frequency where there may be extra sound generated by the treatment. Nevertheless the amount of apparent extra noise here is much less than at 5100 rpm. If there is indeed extra noise generation by the flow interacting with the treatment it seems reasonable to expect the effect to increase rather than decrease with duct Mach number. One possible explanation for this apparent conflict is that MPT's become a significant part of the spectrum as speed is increased. Thus MPT's may mask the broadband increase.

This section has shown in-duct acoustic probe measurements taken at two axial stations. For all cases (configurations, speeds, and positions) there were tones at multiples of the shaft rotation frequency, although these tones were much stronger at 6200 rpm than at 5100 rpm. In general, these tones are stronger at the probe position nearest the fan and the outer wall; there is also a decrease of the blade-passing tone as the probe was moved radially inward from the outer wall. This effect was more pronounced at the higher speed, and it indicates a high concentration of sound energy near the outer wall. These details will be discussed further in connection with the comparisons of estimated and measured suppressor performance. Finally, the comparisons of simulated hard wall and soft wall in-duct narrow-band spectra indicate that extra noise may have been generated at frequencies below about 800 hertz when the treatment was made active.

COMPARISON OF ATTENUATION ESTIMATES AND MEASURED RESULTS

It is reasonable to inquire how well the measured noise reductions compare with expected performance. This question is answered by comparisons of measured and estimated sound reductions in terms of PWL insertion loss spectra. The measured PWL reduction (or insertion loss) was determined for a given treated configuration from the measured PWL spectrum for the baseline inlet configuration. The estimated PWL reduction was calculated for the known suppressor design using theoretical results as modified by empirical adjustments from fan noise suppressor tests as described in reference 3. It could be argued that the proper baseline should be a hard three-ring inlet configuration because theoretical analyses really apply specifically to the case of treating an existing duct. But a designer wants to know the effect of inserting and activating

the rings. The empirically adjusted theoretical predictions were based on this premise. By this means, the predictions account for the total effect of inserting the rings.

As was shown in figure 4, the three-ring inlet noise suppressor has four parallel acoustic passages, I, II, III, and IV. The three outer passages have annular cross sections, and the inner (IV) passage has a circular cross section. In principle the same theoretical equations apply to all four passages. But in practice it is easier to analyze the three outer passages by rectangular duct approximations and to analyze the inner passage as a circular duct.

The noise reduction estimates here were based on the parametric relations in reference 3. In that report the total inlet performance estimate was approximated by the estimated performance for a single passage of the parallel combination of passages. This approximation implied either that the other parallel passages acted similarly or that the most significant part of the noise was confined to the single passage analyzed.

Use of the noise attenuation calculation methods presented in reference 3 resulted in the spectral comparisons of attenuation shown in figure 15. The experimental data and therefore the analysis are for the partially taped inlet configuration of figure 4(c). The single-passage estimate was made for passage I, the outermost passage, because it has the largest cross-sectional area and therefore the largest part of the sound power transmission. It is clear from figure 15 that the single-passage prediction overestimated the measured noise reductions at both speeds. But it is encouraging that there is a good comparison between the predicted and measured spectral shapes and, in particular, that the frequencies of peak attenuation are well predicted. As an aside, it is interesting to examine the effect of using the three-ring simulated baseline for the attenuation data presented here. Figure 10 showed that the three-ring simulated baseline configuration had higher noise levels everywhere except at the blade-passage frequency at 5100 rpm and at all frequencies above the blade passage frequency at 6200 rpm. The use of this baseline would increase the measured attenuations in these ranges and would therefore improve the results of the comparisons between estimates and data.

The overestimate by the single-passage prediction motivated further examination of the other parallel passages. It is apparent from figure 4 that the passages are not alike. In particular passage III has less treatment than passages I and II, and part of the treated surface in passage III is opposed by the acoustically hard surface of the trailing edge of the inner-ring. Furthermore, the inner passage (IV) has a cylindrical cross section and less treatment than any of the others. Therefore, passages III and IV should provide less noise reduction than passages I and II. Assuming that the parallel passages act independently to reduce the noise that they receive, it is a simple matter to estimate the attenuation spectrum to be expected from each passage. These estimates were calculated using the methods of reference 3 and are presented in figure 16 for the two speeds 5100 and 6200 rpm. As seen in figure 16 the three outer annular passages are

estimated to yield good attenuation levels, but the inner cylindrical passage is estimated to yield a very poor attenuation. Therefore, the inner passage would appear to be a noise leak, and this observation may help to explain the discrepancy between the estimates and the data of figure 15.

To further explore this possibility, it is necessary to examine the way that the individual parallel-passage attenuation spectra combine. This means that the sound energy spectrum incident on any given passage must be known. That sound energy spectrum is then attenuated according to the passage's individual characteristics. The overall sound power reduction spectrum would then be calculated by comparing the integrated sum of the energy entering all the passages with the integrated sum of the energy leaving all the passages. Thus, the effects taken into consideration included area weighting, radial sound intensity distribution, and individual passage power attenuation spectra.

In the analysis that follows, the sound power in an individual one-third-octave frequency band is considered. To calculate a spectrum, the bands are individually analyzed. The sound power into the parallel passage suppressor is

$$P_{in} = I_{ref} 10^{SPL_1/10} \sum_{i=1}^{N} A_i 10^{-\delta_i/10} \tag{1}$$

where P_{in} is the incident one-third-octave-band sound power in watts, I_{ref} is the reference for sound intensity level (the numerical value is not important here because it later divides out), SPL_1 is the sound pressure level in the outer passage, which is assumed to be representative of the average intensity level there, A_i is the flow area of the i^{th} passage, and δ_i sets the average level in the i^{th} passage relative to SPL, that is,

$$SPL_i = SPL_1 - \delta_i, \qquad \delta_1 \equiv 0 \tag{2}$$

The summation in equation (1) is taken over all N (=4) passages. The selection of passages corresponding to the indices 1, . . ., N is arbitrary. But, for the present, index 1 is the same passage as I of figure 3, 2 is the same as II, etc.

The sound power out of the set of parallel passages is

$$P_{out} = I_{ref} 10^{SPL_1/10} \sum_{i=1}^{N} A_i 10^{-(\delta_i+\Delta_i)/10} \tag{3}$$

where P_{out} is the sound power output (in W), and Δ_i is the sound level reduction (in dB) due to the treated surfaces in the i^{th} passage.

The overall sound power level reduction (attenuation) is then

$$\Delta PWL = PWL_{in} - PWL_{out} \tag{4}$$

The definition of power level gives

$$\Delta PWL = 10 \log \frac{P_{in}}{P_{out}} \tag{5}$$

and finally

$$\Delta PWL = 10 \log \left\{ \frac{\sum_{i=1}^{N} A_i 10^{-\delta_i/10}}{\sum_{i=1}^{N} A_i 10^{-(\delta_i+\Delta_i)/10}} \right\} dB \tag{6}$$

This result yields the power level attenuation in a single one-third-octave frequency band. To calculate a spectrum, the equation must be used at each frequency band of interest.

Several special cases are of interest. The first is the case where $\delta_i = 0$ for all i and where the Δ_i are the same from one passage to another. This is the case where sound pressure levels are uniformly distributed across the acoustic entrance to the liner and the parallel passages all act the same. Equation (6) reduces to

$$\Delta PWL' = \Delta_i \tag{7}$$

which is exactly what we would expect for this simplified case.

A second special case of interest is again one for which $\delta_i \equiv 0$ for all i passages.

$$\Delta PWL'' = 10 \log \left\{ \frac{\sum_{i=1}^{N} A_i}{\sum_{i=1}^{N} A_i 10^{-\Delta_i/10}} \right\} \tag{8}$$

Further specializing, suppose Δ_1, Δ_2, and Δ_3 are large but Δ_4 is small. Then,

$$\Delta PWL'' \cong 10 \log \frac{\sum_{i=1}^{N} A_i}{A_4 10^{-\Delta_4/10}} \tag{9}$$

simplifying

$$\Delta PWL'' = 10 \log \frac{A_t}{A_4} + \Delta_4 \tag{10}$$

where

$$A_t = \sum_{i=1}^{N} A_i$$

The implication of equation (10) is that if all of the parallel sound paths, except one, are made very effective, the overall achievable attenuation is limited by the area ratio and attenuation realized in the exceptional passage. The three-ring inlet here, as a case in point, with the inner cylindrical passage being the exceptional one, would give

$$\Delta PWL'' \cong 10 \log 20 + \Delta_4 \tag{11}$$

Therefore, the overall achievable attenuation would be limited to 13 decibels in the event $\Delta_4 = 0$. This says that even a small ($\sim$5 percent total area) noise leak cannot be allowed when the goal is large attenuations. For the TF-34 inlet liner estimates it was initially assumed that the acoustic input sound intensity was uniform across the duct. Equa-

tion (8) above was programmed for automated computer handling of the repetitious calculations to generate ΔPWL spectra. The result was an area-weighted attenuation spectrum that combined the individual passage spectra of figure 16. A comparison of these area weighted spectra at 5100 and 6200 rpm and the measured spectra is shown in figure 17 for the assumed uniform sound profile. This comparison shows that the poorly performing inner passage penalizes the overall estimate too much because the overall estimate is now low and the shape comparison is poorer.

In the general case the sound pressure level profile tends to be nonuniform, high at the outer wall and dropping off toward the center, as was seen from the narrow band in-duct spectra of figures 13 and 14. Therefore, $\delta_i \neq 0$, and equation (6) must be used for the calculation. It seems obvious, and it can be shown from equation (6), that a case with a sound profile that has a low sound level entering a poorly attenuating parallel passage does not allow as much noise to escape as would be indicated by the calculations for the uniform case.

To insert the actual sound profiles into equation (6), the taped configuration narrow-band spectra of figures 13 and 14 were converted to one-third-octave band spectra using well known conversion formulas (ref. 12). The narrow-band spectra at PT-1 for the baseline inlet were used for this purpose because it was reasoned that these levels were representative of the true sound entering the hard ring passages and therefore the soft ring as well. By contrast it was felt that PT-2 was in the acoustic near field of the rotor and that the PT-2 results therefore should not be used for this purpose.

The one-third-octave band spectra at PT-1 computed as discussed above are shown in figure 18. Points to observe are that the spectra are similar in shape to the far-field power spectra (fig. 9) and the maximum angle sound pressure level spectra (fig. 8). In fact, the far-field power level spectra when mathematically translated to the cross-sectional area of the inlet shows quite good agreement with the spectra of figure 18, except at frequencies below about 800 hertz where the in-duct probe was apparently measuring sound that did not reach the far field. Figure 18 also shows that for most frequencies the sound pressure level was highest nearest the outer wall and the sound levels decreased toward the centerline. This effect was more pronounced at the higher speed, 6200 rpm. The spectra of figure 18 were assumed to be the average sound pressure levels in each of the respective passages. Recall that the probe locations (PT-1) were at the centers of passages I and II and at the half-radius location in passage IV. For the calculations to follow the spectrum at the center of passage III was interpolated from the other three spectra.

Accounting for the measured sound profile in equation (6) led to the estimated PWL reduction spectra shown in figure 19 where they are compared with the measured data. The estimated spectra based on the measured input sound profile are in reasonable agreement with the data at 6200 rpm, (fig. 19(b)), although somewhat different in band-

width character. The irregular shapes of the predicted spectra resulted mainly from the irregular shapes of the input sound level spectra of figure 18. The agreement between prediction and measurement was not so good at 5100 rpm as it was at 6200 rpm. The reason for this discrepancy is not clear. It is possible that the inner cylindrical passage behavior is not well modeled by the present method. The attenuation spectra shape predicted in this inner passage did strongly affect the shape of the area-weighted overall prediction. In particular the presence of spinning modes in this inner duct could allow greater attenuation rates than were accounted for by the present nonspinning mode method. This would mean that the inner passage was less of a noise leak than presently estimated.

The major conclusion to be drawn from this series of comparisons is that single-duct approximations of performance (for parallel-combination ducts) can be misleading and that cross-duct distributions of source sound intensity significantly affect performance predictions for the integrated system. The best agreement between predictions and data was achieved when all of these effects were taken into account. But it appears that, in the present case, suppressor bandwidth predictions were more optimistic than justified. Further work is needed to understand why this occurred.

Liner Length Test Results and Comparisons with Estimates

Further experimental tests were performed in which the active treated length was varied. For all these configurations the outer cowl wall was partly taped over (to simulate hard-wall conditions) at axial locations beyond the extremities of the active portions of the splitters. The inlet liner arrangements for these tests were shown in figure 4. The first case (fig. 4(a)) had an active length of 17.8 centimeters (7.0 in.) on each surface, referred to as nominally quarter active herein. The next case (fig. 4(b)) had an active length of 36.8 centimeters (14.5 in.) in each passage, referred to as nominally half active. Finally, the third case (fig. 4(c)) had the full length active in each passage. This was the case discussed in previous sections. Note that it would be improper to use the stated nominal fractions of lengths to plot attenuation against length, because the fractions are not the same in all passages. Furthermore, it would be improper to plot attenuations against length-to-height ratio because that parameter also varies from one passage to another. For example, in the number III passage part of the lined surfaces have acoustically hard surfaces on opposing walls, thus changing the effective value of length-to-height ratio from the nominal value. Finally, it would probably be improper to expect that the system attenuation would, for example, vary linearly with treated length (as the present estimating procedure assumes for a single passage), because the overall attenuation is a complicated function of the sound profile.

The proper way to attempt a generalization about length effects in these tests is to compare the measured spectra at the different lengths with estimated spectra for these same configurations (which were based on area weighting and sound profile considerations), while accounting for the actual configuration in the analysis. The spectral comparisons for the configurations of figure 4 are shown in figure 20. The agreement of the data and the estimate for each configuration is again better at 6200 than at 5100 rpm. The progression of levels with changing length is reasonably well predicted, while, again, the bandwidth character is broader for the estimates than for the data.

Remarks on Comparisons of Measurements and Estimates

The results for the TF-34 three-ring inlet have shown reasonably good agreement between the predictions and the measured data. The predicted bandwidth was broader than that measured, and the predicted maximum attenuation was less than the measured value. However, there was good agreement between the predicted and measured frequency of peak attenuations. These results are in contrast to those presented in reference 3, where the agreement was shown to be very good. The reasons for the differences are not clear, but it has been demonstrated here that the predicted behavior of the inner cylindrical passage can have a powerful effect on the overall inlet prediction. The results presented in reference 3 were for an inlet with an annular inner passage. Furthermore, the acoustic treatments in the parallel passages for that series of tests were designed with the goal of achieving the same attenuations in all passages.

SUMMARY OF RESULTS

Acoustic performance tests were conducted on a three-ring inlet-noise suppressor on a full scale TF-34 engine. The aft noise sources were highly suppressed throughout the test series. Measured results were presented for two engine speeds, 5100 and 6200 rpm, which are representative of low- and high-speed behavior. The data include extensive far-field perceived noise levels (PNL), sound pressure level spectra, sound power level spectra, sound power level attenuation spectra, and a limited amount of probe-measured, in-duct sound pressure level spectra. Estimates of the expected liner performance were compared with the measured power attenuation spectra. The following important results were observed:

1. Reductions of 15 and 19 effective perceived noise decibels maximum on a 152.5 meter (500 ft) sideline occurred at 5100 and 6200 rpm, respectively. These PNL reductions were accompanied by peak sound pressure level reductions exceeding 30 decibels.

2. At 6200 rpm there were significant multiple pure tones in the far spectrum. These tones were significantly reduced by the inlet treatment even though it was not specifically designed for that purpose.

3. The results from the TF-34 inlet test series have shown reasonably good agreement between predictions and the measured data. Frequencies of peak attenuation were in good agreement. The peak attenuations were generally under predicted, while the bandwidth was over predicted.

4. Sound pressure level attenuations showed an orderly progression with treated length across the frequency range of practical interest.

5. In-duct acoustic probe measurements indicated high sound levels near the outer wall and lower levels near the centerline.

6. Both in-duct and far-field acoustic measurements seem to indicate low-frequency noise generation by the liner. Further work is needed to validate this observation.

Lewis Research Center,
National Aeronautics and Space Administration,
Cleveland, Ohio, November 15, 1975,
505-03.

REFERENCES

1. Jones, W. L.; Heidelberg, L. J.; and Goldman, R. G.: Highly Noise-Suppressed Bypass 6 Engine for STOL Application. AIAA Paper 73-1031, Oct. 1973.

2. Coward, W. E.; Smith, E. B.; and Sowers, H. D.: TF34 Quiet Nacelle Near Field Acoustic Test Results. (R73AEG417, General Electric Co.; NAS3-17845.), NASA CR-134604, 1974.

3. Minner, Gene L.; and Rice, Edward J.: Computer Method for Design of Acoustic Liners for Turbofan Engines. NASA TM X-3317, 1976.

4. Edkins, D. P.: Acoustically Treated Ground Test Nacelle for the General Electric TF34 Turbofan. (General Electric Co.; NAS3-14338.), NASA CR-120915, 1972.

5. Rice, Edward J.; Feiler, Charles E.; and Acker, Loren W.: Acoustic and Aerodynamic Performance of a 6-Foot-Diameter Fan for Turbofan Engines. III - Performance with Noise Suppressors. NASA TN D-6178, 1971.

6. Montegani, Francis J.: Noise Generated by Quiet Engine Fans. I - Fan B. NASA TM X-2528, 1972.

7. Montegani, Francis J.; Schaefer, John W.; and Stakolich, Edward G.: Noise Generated by Quiet Engine Fans. II - Fan A. NASA TM X-3066, 1974.

8. Montegani, Francis J.: Some Propulsion System Noise Data Handling Conventions and Computer Programs Used at the Lewis Research Center. NASA TM X-3013, 1974.

9. Dittmar, James H.; and Groeneweg, John F.: Effect of Treated Length on Performance of Full Scale Turbofan Inlet Noise Suppressors. NASA TN D-7826, 1974.

10. Rice, E. J.: Spinning Mode Sound Propagation in Ducts with Acoustic Treatment. Presented at the Eighty-eighth Meeting of the Acoustical Society of America, St. Louis, Mo., Nov. 5-8, 1974. (NASA TN D-7913, 1975.)

11. Saule, Arthur V.: Some Observations about the Components of Transonic Fan Noise from Narrow-Band Spectral Analysis. NASA TN D-7788, 1974.

12. Harris, Cyril M., ed.: Handbook of Noise Control. McGraw-Hill Book Co., Inc., 1957.

TABLE I. - TF-34 DESIGN AND PERFORMANCE

(a) Design parameters

Fan diameter, m (in.)	1.12 (44)
Fan hub diameter, m (in.)	0.478 (18.8)
Number fan rotor blades	28
Number fan stator vanes	44

(b) Measured sea level static standard day performance

Inlet	Rotative speed, rpm	Thrust		Fan pressure ratio	Weight flow		Bypass ratio	Fan tip speed	
		N	lb		$\frac{kg}{sec}$	$\frac{lb}{sec}$		$\frac{m}{sec}$	$\frac{ft}{sec}$
Unsuppressed	6800	40 900	9200	1.480	151	332	6.7	398	1307
Fully treated	6930	35 700	8040	1.473	149	328	6.71	406	1332
	6200	27 500	6180	1.364	134	295	7.07	363	1191
	5100	16 700	3760	1.224	109	240	7.40	299	980

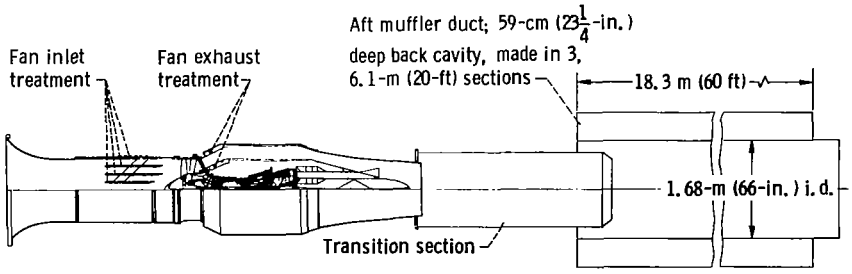

Figure 1. - Acoustically treated TF-34 engine installation.

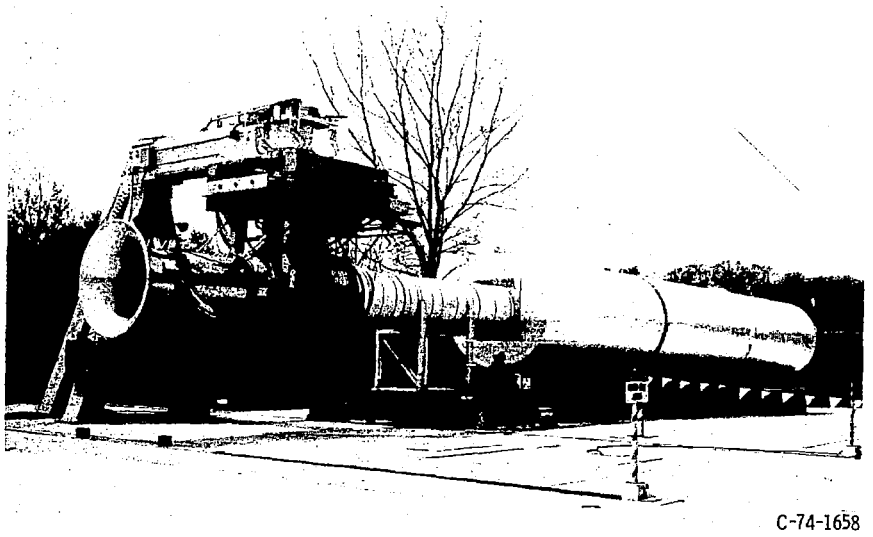

C-74-1658

Figure 2. - TF-34 engine on test stand with aft duct extension and muffler.

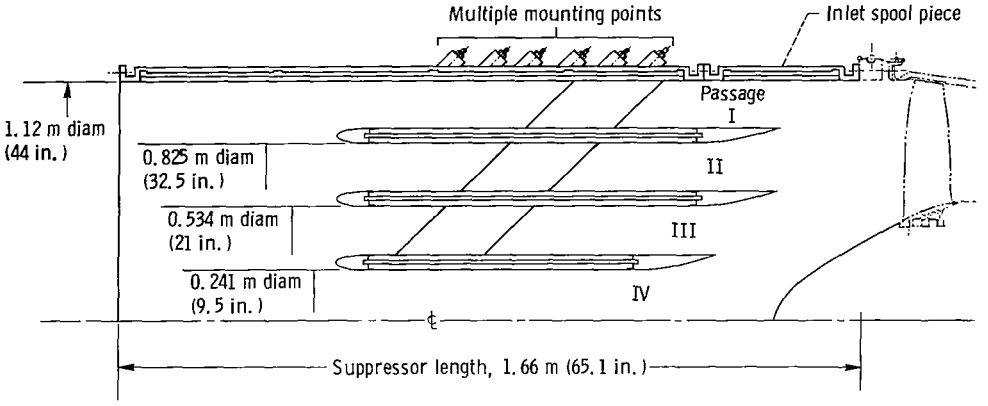

Part	Total treated length, m (in.)	Passage height, m (in.)
Outer wall	1.33 (52.5)	0.114 (4.5)
Outer ring	.71 (28.)	.114 (4.5)
Middle ring	.71 (28.)	.114 (4.5)
Inner ring	.57 (22.5)	.241 (9.5) diam

Figure 3. - TF-34 fully treated inlet suppressor. Acoustic treatment: perforate face sheet (open area, 6.8 percent); honeycomb depth, 1.2 centimeters (0.480 in.); sheet thickness, 0.05 centimeter (0.02 in.); hole size, 0.127 centimeter (0.05 in.); splitter thickness, 3.2 centimeters (1.25 in.).

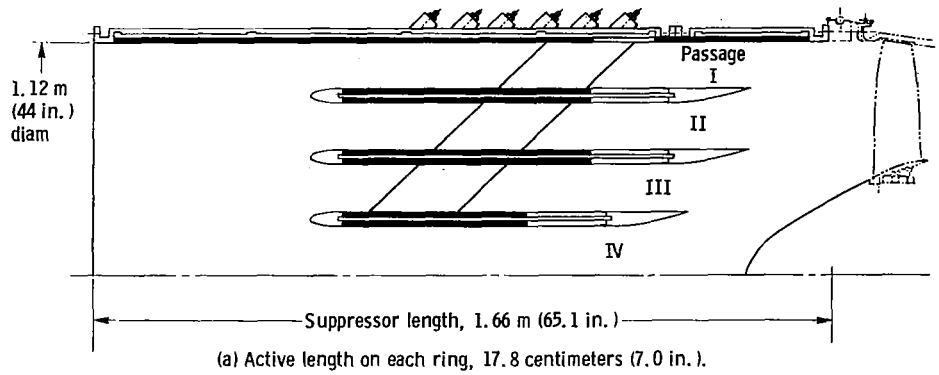

(a) Active length on each ring, 17.8 centimeters (7.0 in.).

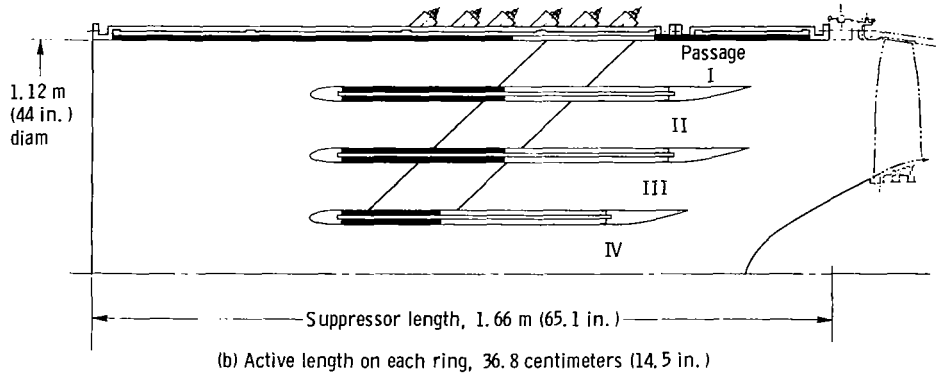

(b) Active length on each ring, 36.8 centimeters (14.5 in.)

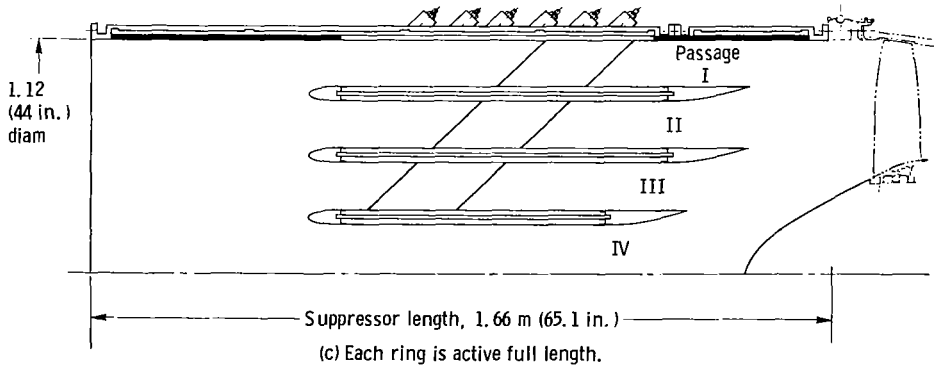

(c) Each ring is active full length.

Figure 4. - TF-34 inlet liner length variations. Nonblackened portions indicate acoustically active parts of liner.

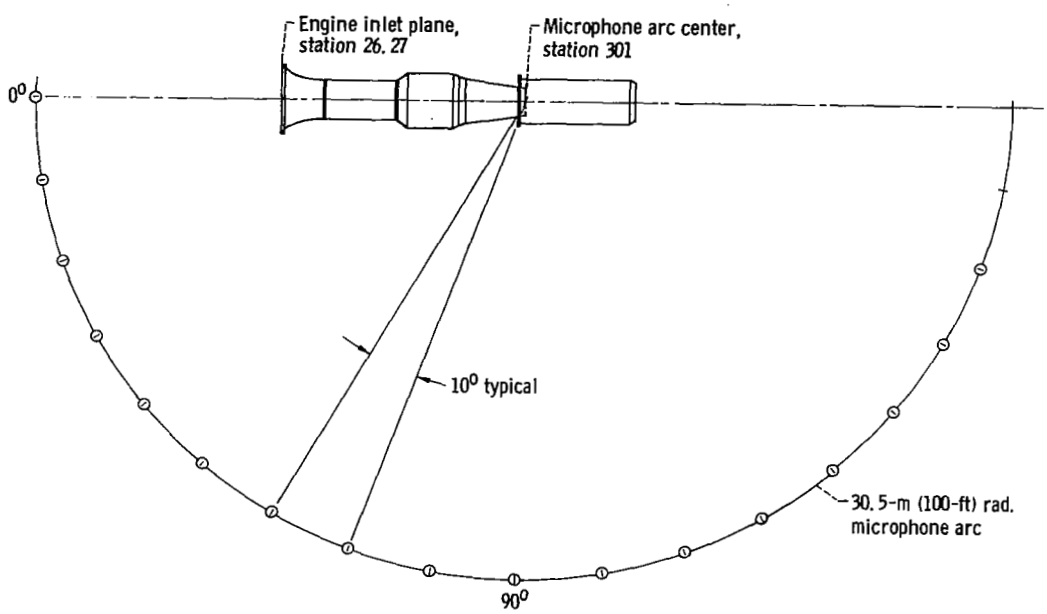

Figure 5. - Plan view of engine test site for inlet series of experiments.

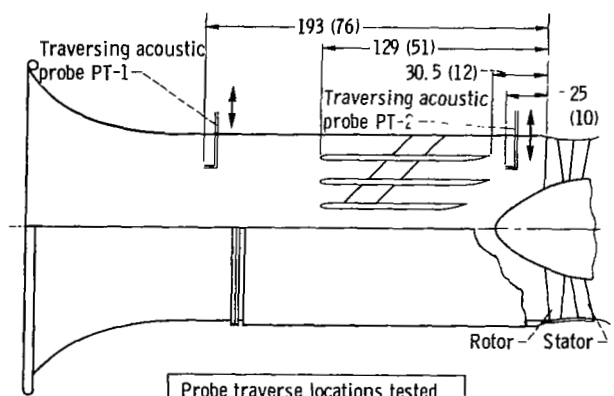

Probe traverse locations tested, cm (in.)	
PT-1 immersion	PT-2 immersion
5.7 (2.25)	5.7 (2.25)
20. (8)	20. (8)
49.9 (19.6)	41. (16.1)

Figure 6. - Cutaway of inlet showing traversing acoustic probe placements. (All dimensions are in cm (in.).)

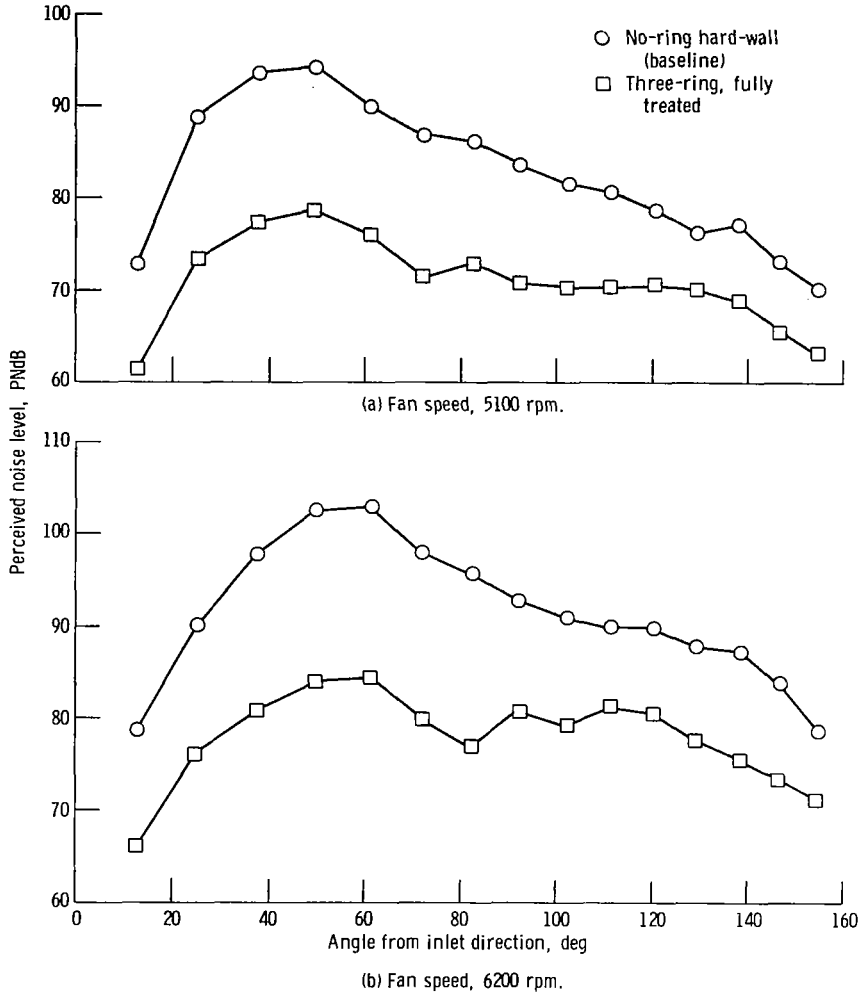

(a) Fan speed, 5100 rpm.

(b) Fan speed, 6200 rpm.

Figure 7. - Angular distribution of perceived noise level on 152.5-meter (500-ft) sideline.

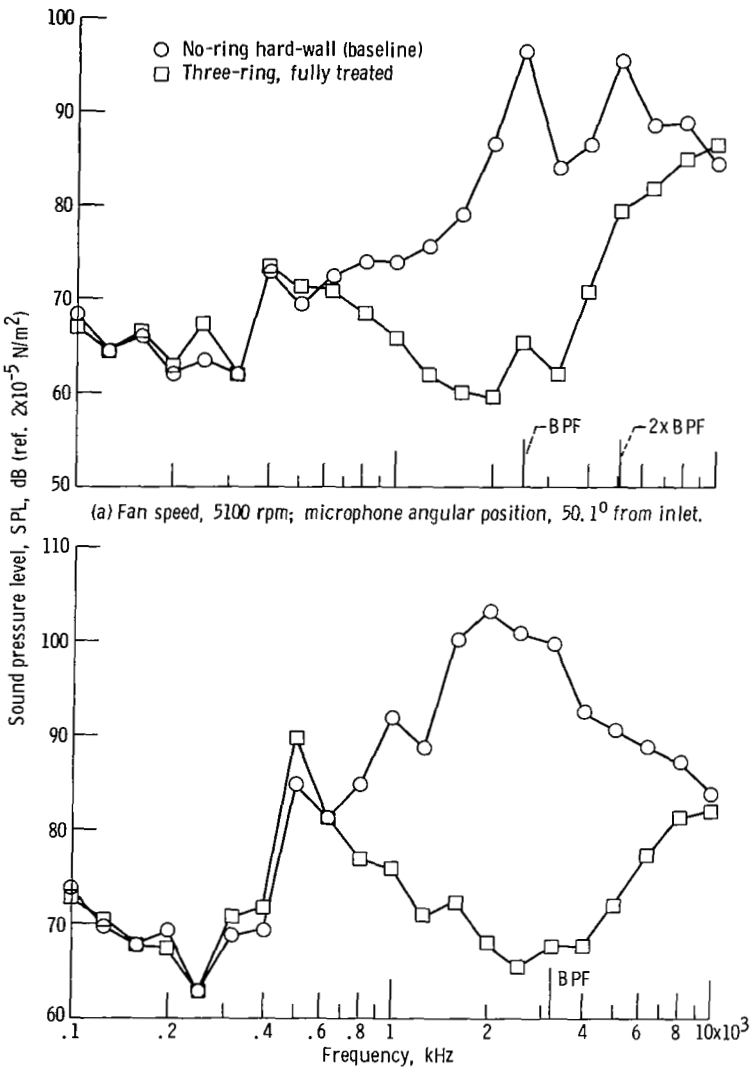

(a) Fan speed, 5100 rpm; microphone angular position, 50.1^0 from inlet.

(b) Fan speed, 6200 rpm; microphone angular position, 61.6^0 from inlet.

Figure 8. - Sound pressure level spectra at angle of maximum perceived noise level. Microphone array radius, 30.5 meters (100 ft).

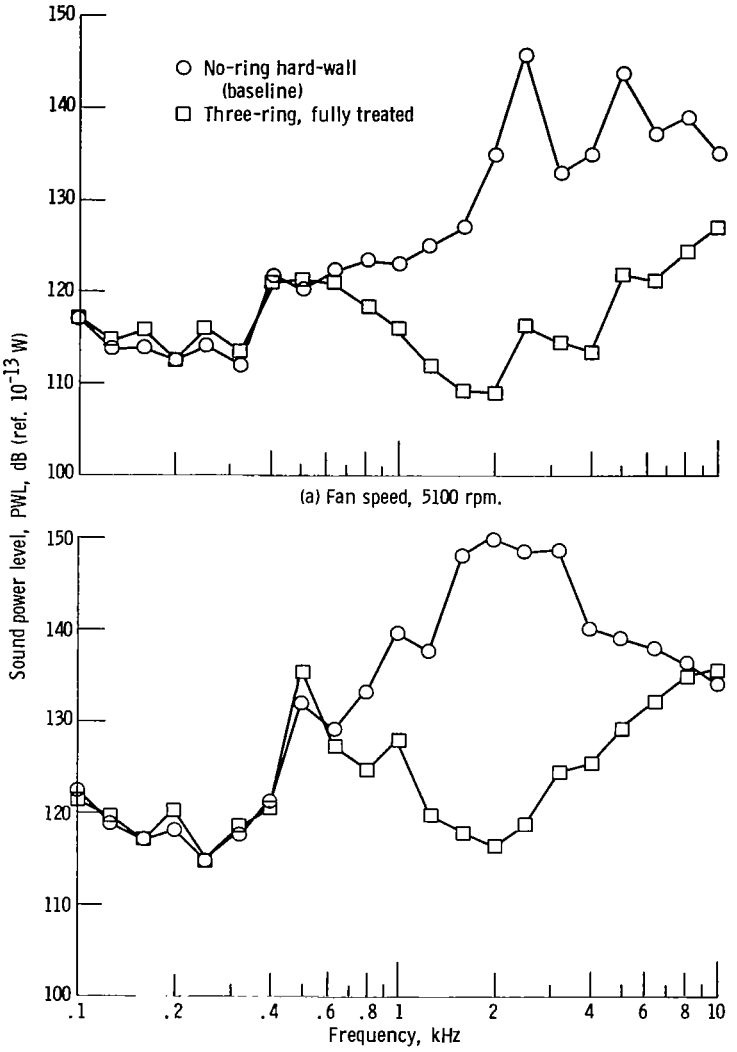

(a) Fan speed, 5100 rpm.

(b) Fan speed, 6200 rpm.

Figure 9. - Far-field measured inlet power spectra.

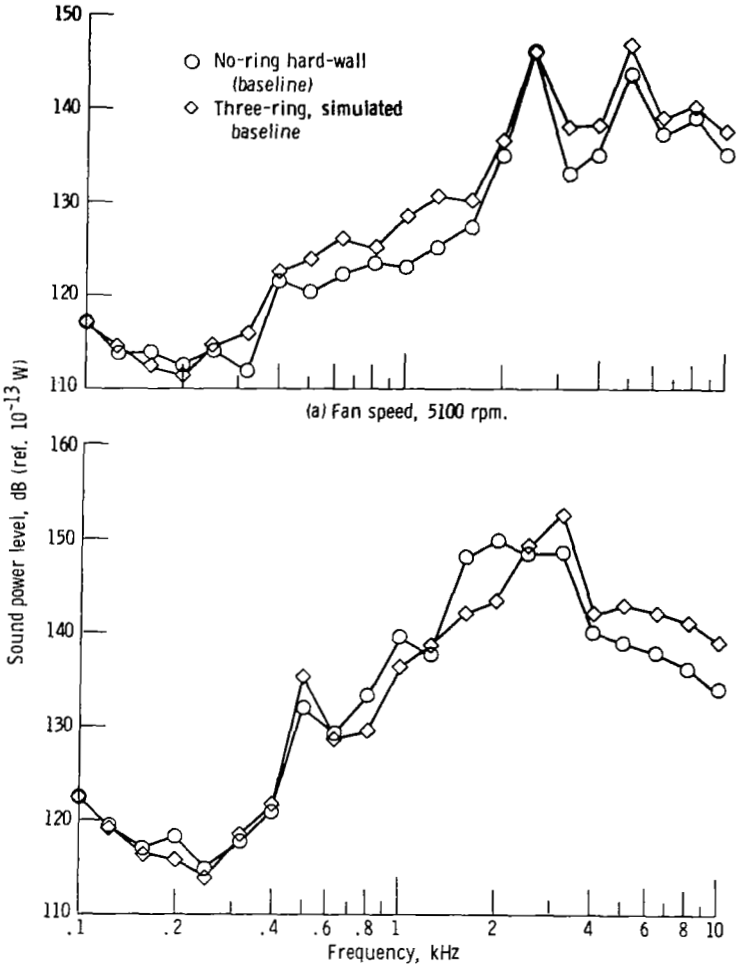

Figure 10. - Far-field measured inlet power spectra of no-ring and three-ring hard inlets.

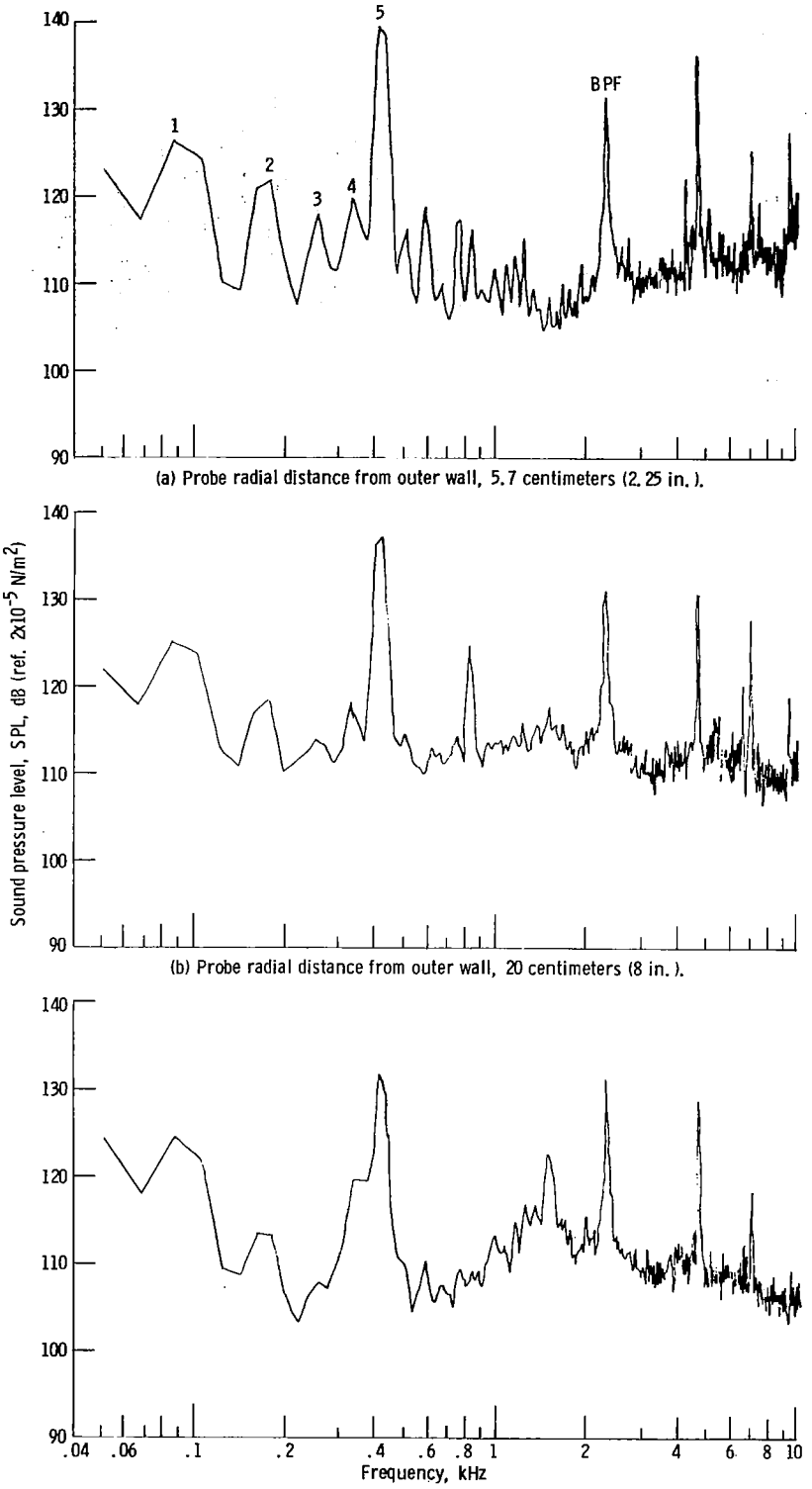

(a) Probe radial distance from outer wall, 5.7 centimeters (2.25 in.).

(b) Probe radial distance from outer wall, 20 centimeters (8 in.).

(c) Probe radial distance from outer wall, 41 centimeters (16.12 in.).

Figure 11. - 20 Hertz narrow-band sound pressure level spectrum at PT-2 probe location. Soft, two-outer-ring inlet; fan speed, 5100 rpm.

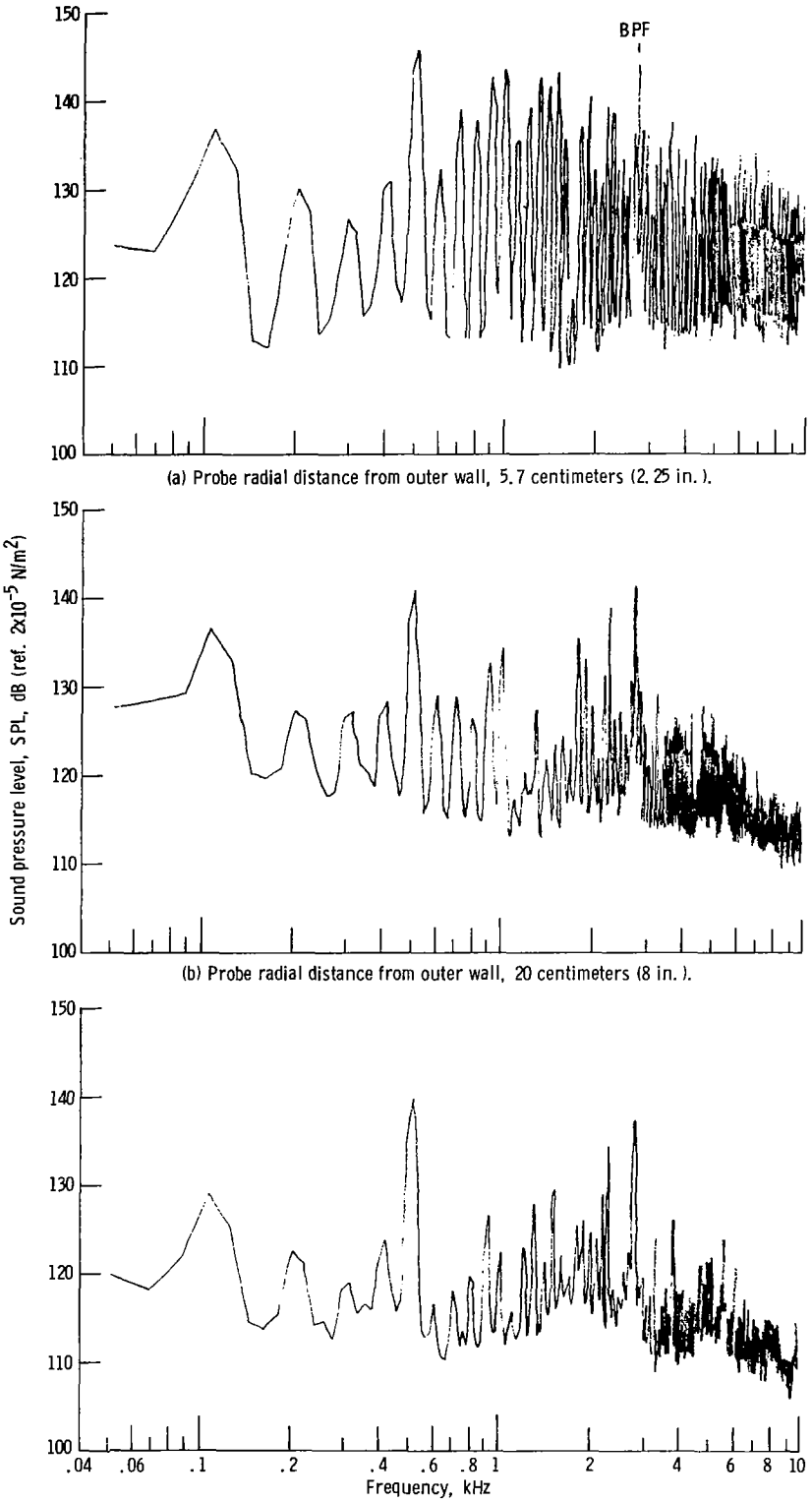

(a) Probe radial distance from outer wall, 5.7 centimeters (2.25 in.).

(b) Probe radial distance from outer wall, 20 centimeters (8 in.).

(c) Probe radial distance from outer wall, 41 centimeters (16.12 in.).

Figure 12. - 20 Hertz narrow-band sound pressure level spectrum at PT-2 probe location. Soft, two-outer-ring inlet; fan speed, 6200 rpm.

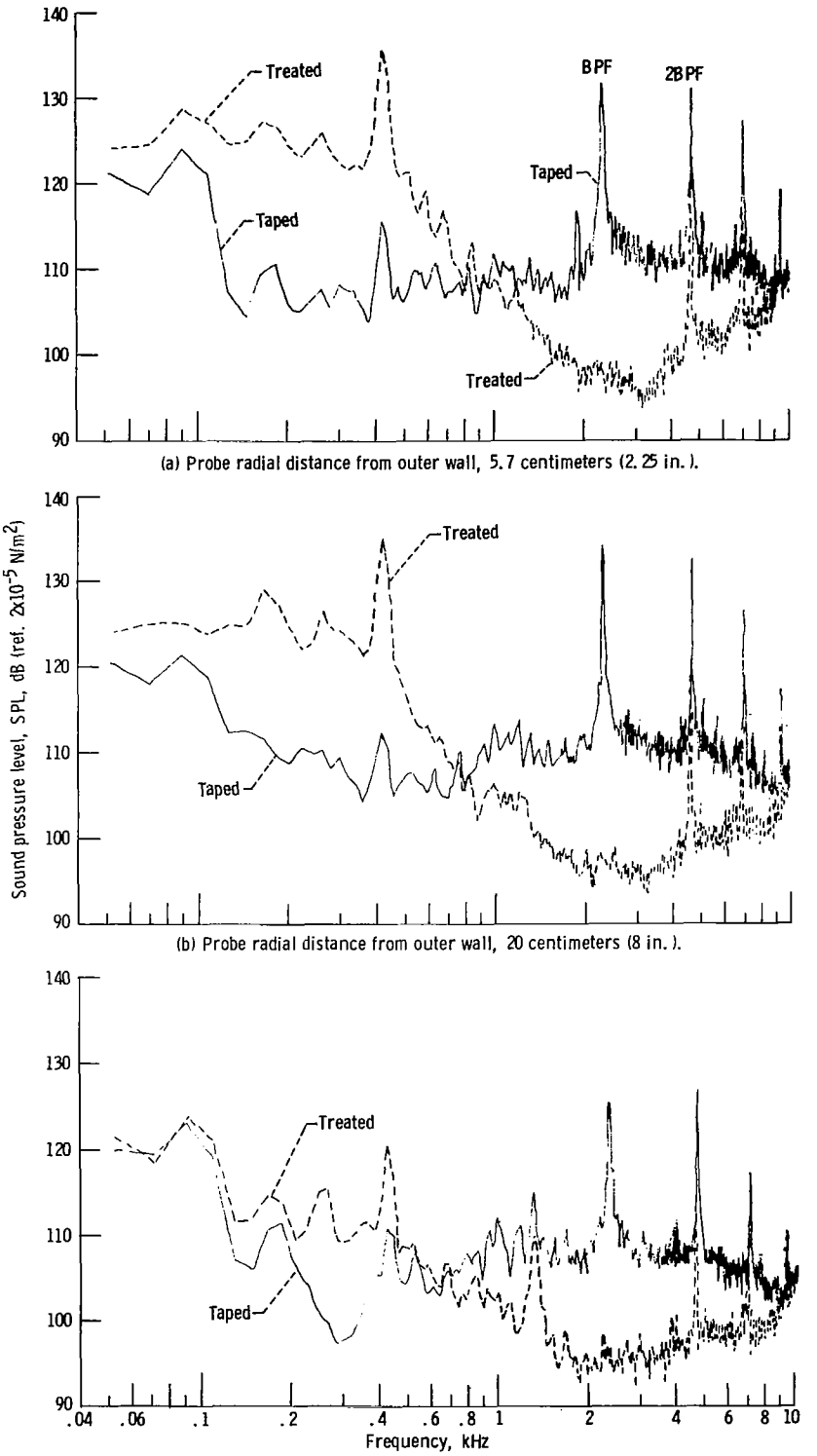

(a) Probe radial distance from outer wall, 5.7 centimeters (2.25 in.).

(b) Probe radial distance from outer wall, 20 centimeters (8 in.).

(c) Probe radial distance from outer wall, 49.9 centimeters (19.62 in.).

Figure 13. - 20 Hertz narrow-band SPL spectra at PT-1 probe location. Three-ring inlet; fan speed, 5100 rpm.

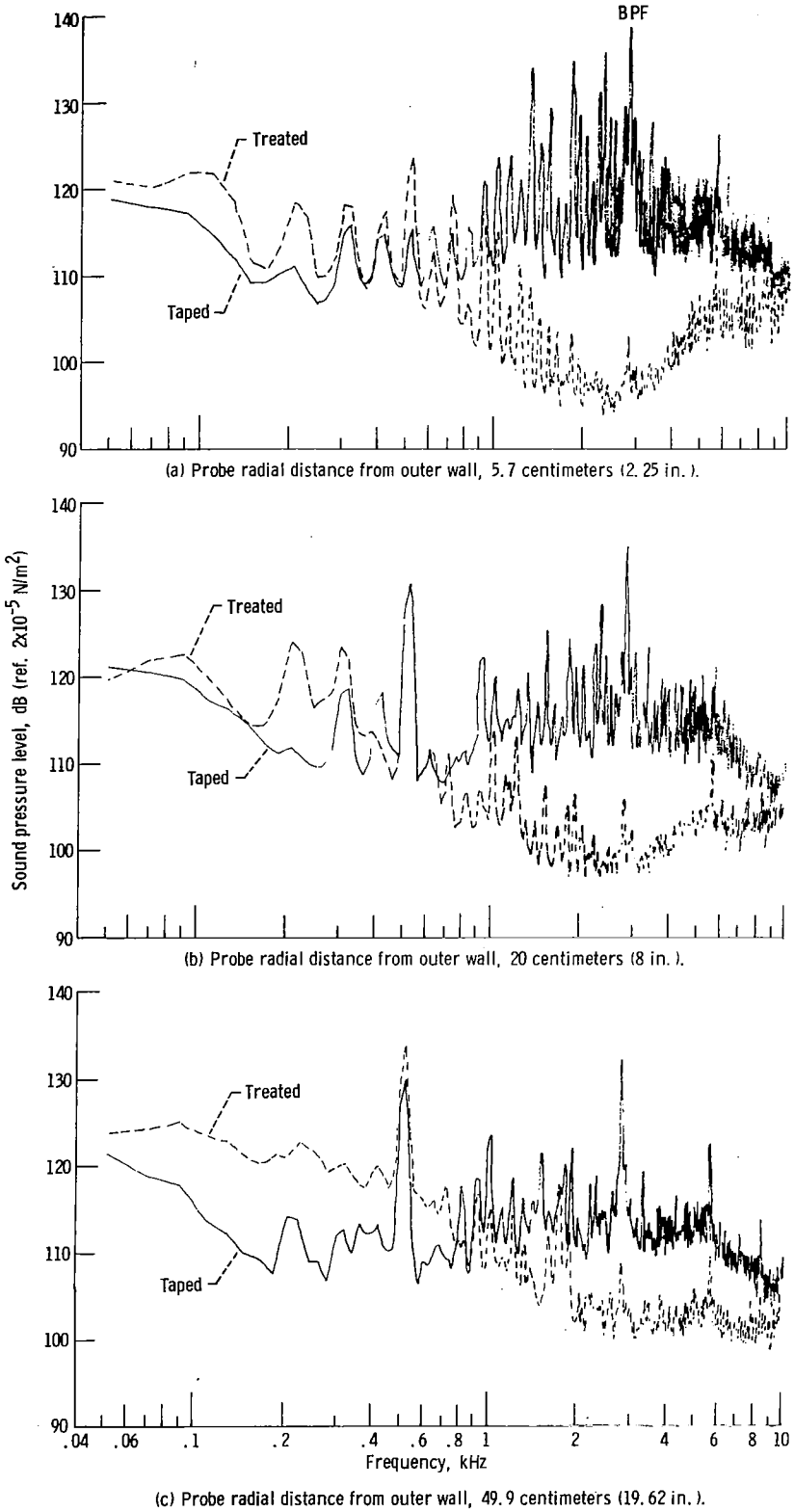

(a) Probe radial distance from outer wall, 5.7 centimeters (2.25 in.).

(b) Probe radial distance from outer wall, 20 centimeters (8 in.).

(c) Probe radial distance from outer wall, 49.9 centimeters (19.62 in.).

Figure 14. - 20 Hertz narrow-band SPL spectra at PT-1 probe location. Three-ring inlet; fan speed, 6200 rpm.

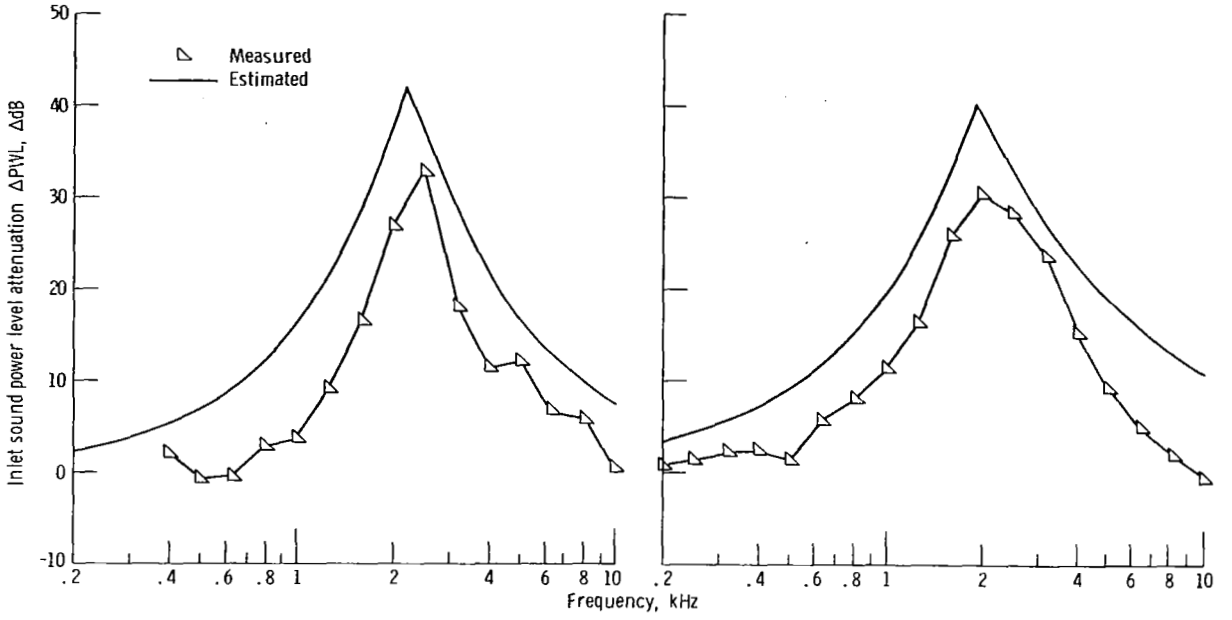

(a) Fan speed, 5100 rpm.

(b) Fan speed, 6200 rpm.

Figure 15. - Attenuation comparison of measured and estimated results for passage I. Configuration shown in figure 4(c).

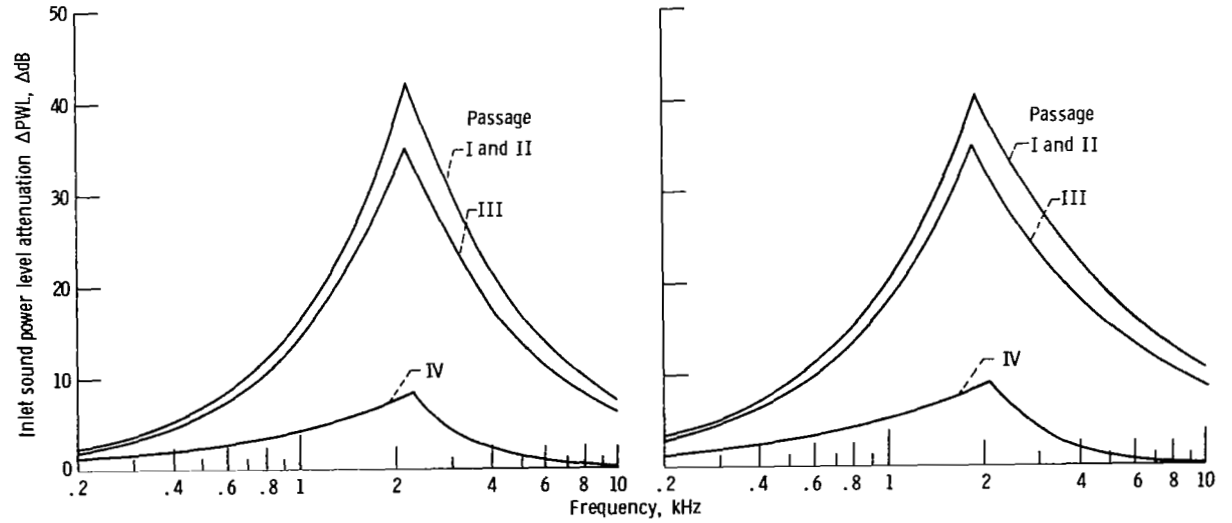

(a) Fan speed, 5100 rpm.

(b) Fan speed, 6200 rpm.

Figure 16. - Sound power attenuation estimates for individual passages of TF34 three-ring inlet. Configuration shown in figure 4(c).

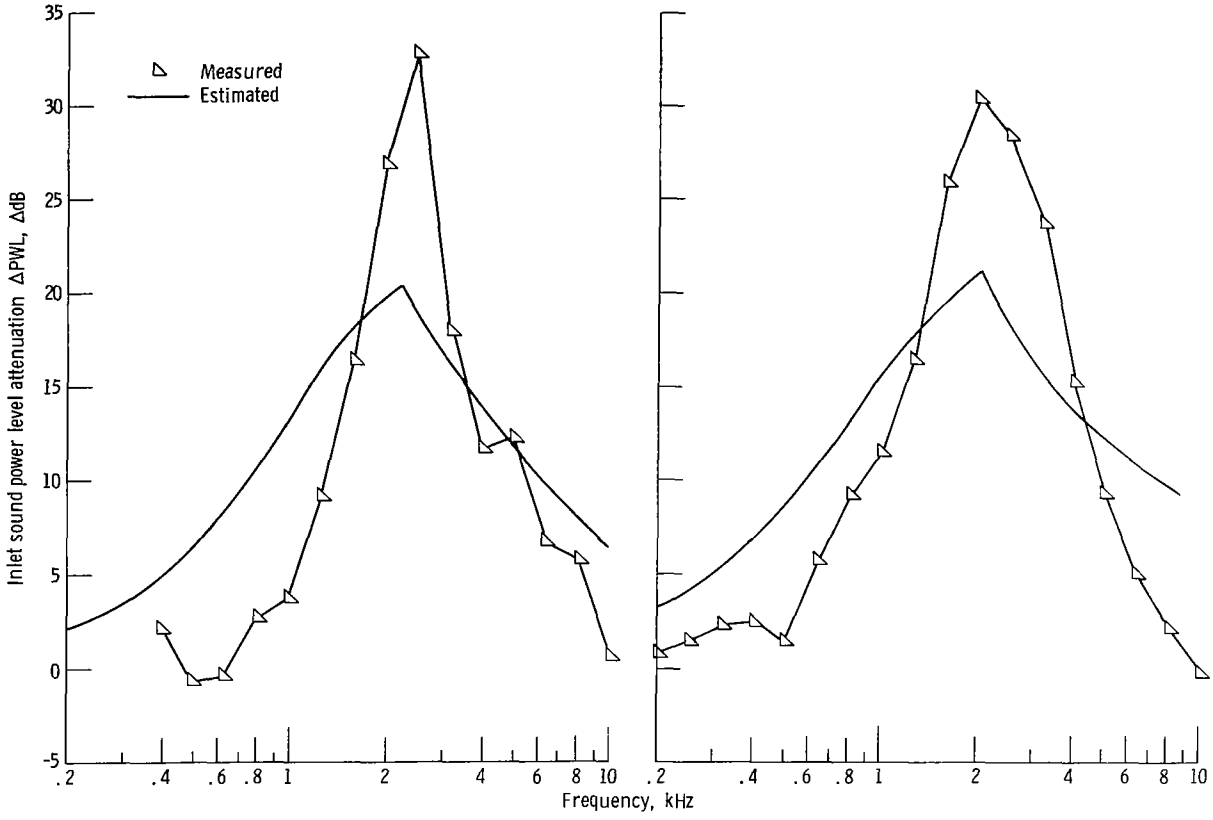

(a) Fan speed, 5100 rpm.

(b) Fan speed, 6200 rpm.

Figure 17. - Comparison of measured and estimated attenuation assuming uniform sound profile in duct. Configuration shown in figure 4(c).

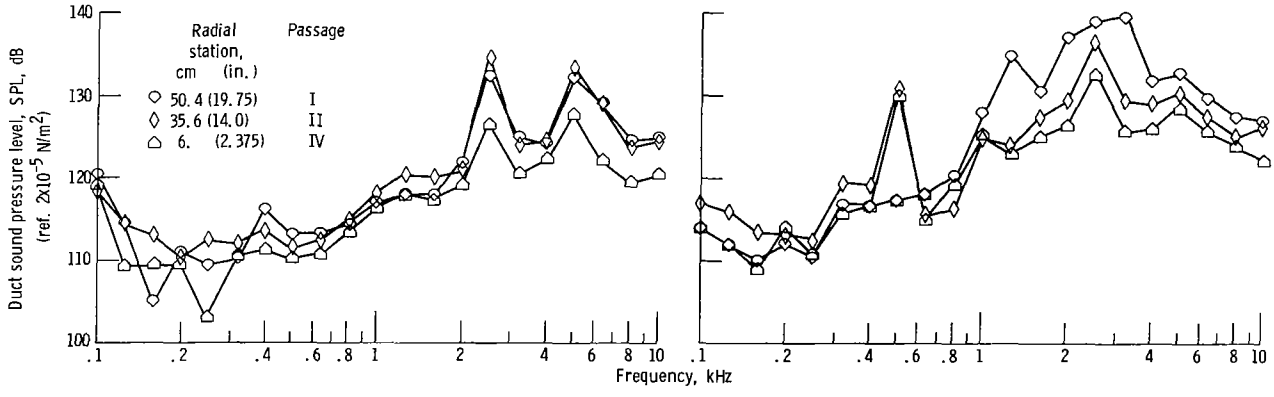

(a) Fan speed, 5100 rpm.

(b) Fan speed, 6200 rpm.

Figure 18. - Spectra of sound pressure level at three radial stations in duct (PT-1).

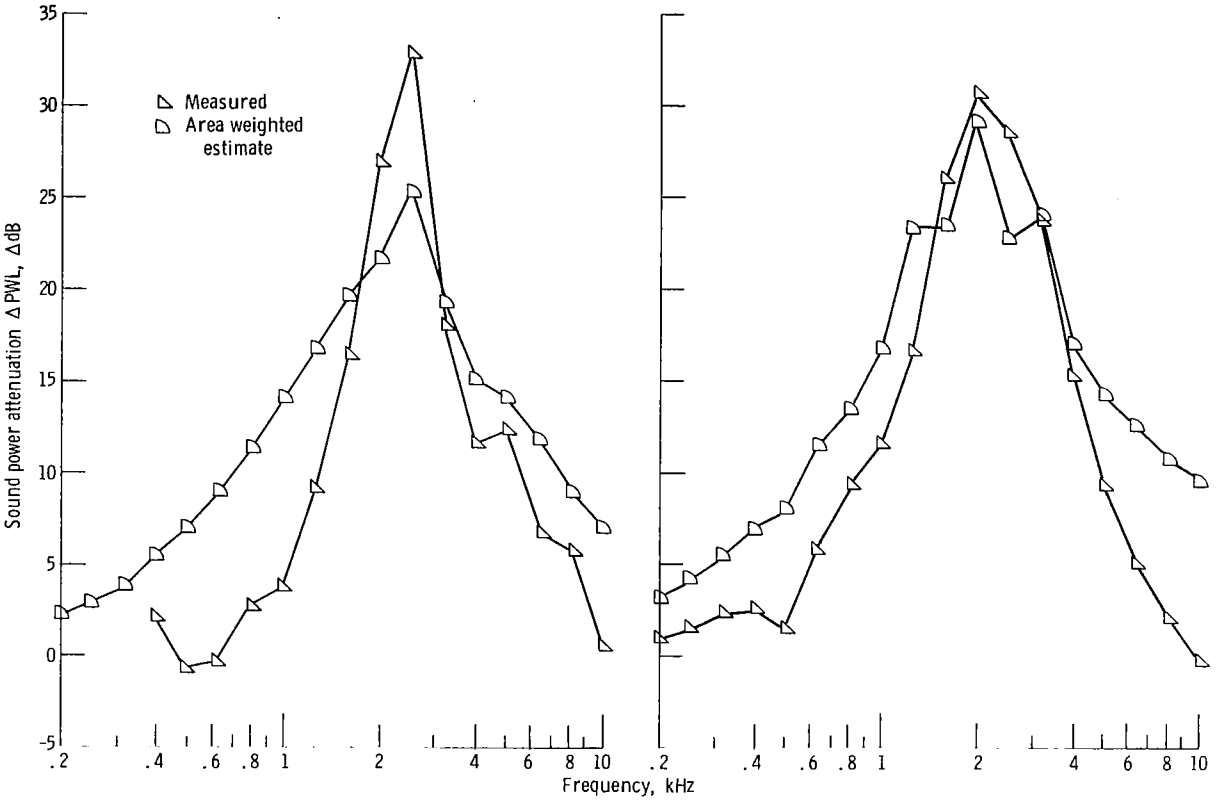

(a) Fan speed, 5100 rpm.

(b) Fan speed, 6200 rpm.

Figure 19. - Three-ring inlet sound power attenuation. Duct spectra accounted for in estimate. Configuration shown in figure 4(c).

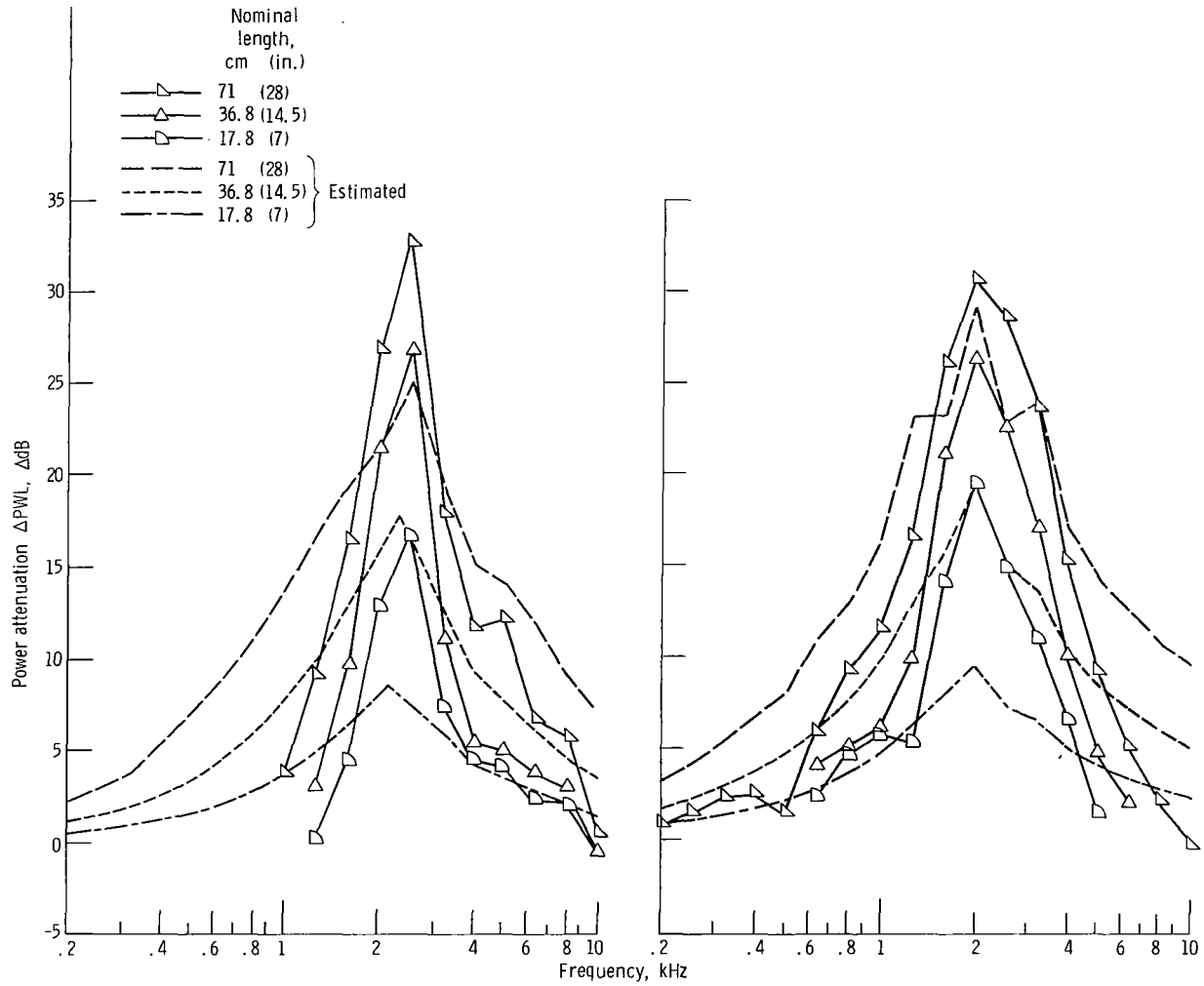

(a) Fan speed, 5100 rpm.

(b) Fan speed, 6200 rpm.

Figure 20. - Effect of treated length on liner measured and estimated sound power attenuation. Configurations shown in figure 4.